Regular paper

Running title: A facultative auxin transporter ABCB21

Corresponding author; Kazufumi Yazaki
Address: Laboratory of Plant Gene Expression, Research Institute for Sustainable Humanosphere, Kyoto University, Gokasho, Uji 611-0011, Japan
Tel +81-774-38-3617
Fax +81-774-38-3623
E-mail: yazaki@rish.kyoto-u.ac.jp

Subject Areas; growth and development, membrane and transport

Number of black and white figures are 6

Number of color figures and tables are 1

Title:

***Arabidopsis* ABCB21 is a facultative auxin im/exporter regulated by cytoplasmic auxin concentration**

Authors:

Yoshihisa Kamimoto[1], Kazuyoshi Terasaka[2], Masafumi Hamamoto[1], Kojiro Takanashi[1], Shoju Fukuda[1], Nobukazu Shitan[1], Hideyuki Suzuki[3], Daisuke Shibata[3], Bangjun Wang[4, 7], Stephan Pollmann[5,6], Markus Geisler[4,7], and Kazufumi Yazaki[1§]

Institution address:

[1] Laboratory of Plant Gene Expression, Research Institute for Sustainable Humanosphere, Kyoto University, Gokasho Uji 611-0011, Japan

[2] Graduate School of Pharmaceutical Sciences, Nagoya City University, Japan

[3] Kazusa DNA Research Institute, 2-6-7 Kazusakamatari, Kisarazu, Chiba 292-0818, Japan

[4]Institute of Plant Biology, Basel–Zurich Plant Science Center, University of Zurich, CH-8007 Zurich, Switzerland

[5]Ruhr-Universität Bochum, Lehrstuhl für Pflanzenphysiologie, Germany

[6] Present address: Centro de Biotecnología y Genómica de Plantas, Campus de Montegancedo, 28223 Pozuelo de Alarcón, Madrid, Spain

[7] Present address: University of Fribourg, Department of Biology

Plant Biology, CH-1700 Fribourg, Switzerland

Abbreviation:

ABC, ATP-binding cassette; GUS, beta-glucuronidase; IAA, indoleacetic acid; LR, lateral root; NAA, Naphthalene acetic acid; NBD, nucleotide-binding domain; ORF, open reading frame; PGP, P-glycoprotein; RNAi, RNA interference; TMD, transmembrane domain; UTR, untranslated region.

Footnotes:

This work was supported by a Grant-in-Aid for Scientific Research 17027016, 19060016 and 20061018 (to K.Y.), by the Swiss National Science Foundation, *Pole de Recherche* of the University of Fribourg and FOBI (all to M. G.), and a grant from the PM Project by NEDO (to S. D. and H. S.).

[§]Corresponding author; e-mail yazaki@rish.kyoto-u.ac.jp; fax +81-774-38-3623

**Abstract**

The phytohormone auxin is critical for plant growth and many developmental processes. Members of the P-glycoprotein (PGP/ABCB) subfamily of ABC transporters have been shown to function in the polar movement of auxin by transporting auxin over the plasma membrane in both monocots and dicots. Here, we characterize a new *Arabidopsis* member of the ABCB subfamily, ABCB21/PGP21, a close homolog of ABCB4, for that conflicting transport directionalities have been reported. *ABCB21* is strongly expressed in the abaxial side of cotyledon and in junctions of lateral organs in the aerial part, whereas in roots it was specifically expressed in pericycle cells. Membrane fractionation by sucrose density gradient centrifugation followed by western blot showed that ABCB21 is a plasma membrane-localized ABC transporter. Transport assay with *Arabidopsis* protoplasts suggested that ABCB21 was involved in IAA transport in an outward direction, while NAA was a less preferable substrate for ABCB21. Further functional analysis of ABCB21 using yeast im- and export assays showed that ABCB21 mediates the NPA-sensitive translocation of auxin in an inward direction when cytoplasmic IAA concentration is low, whereas this transporter mediates outward transport under high internal IAA. Increase in the cytoplasmic IAA concentration by pre-loading of IAA into yeast cells abolished the IAA uptake activity by ABCB21 as well as ABCB4. These findings suggest that ABCB21 functions as a facultative im-/exporter controlling auxin concentrations in plant cells.

Key words: ABC protein, ABCB21, *Arabidopsis thaliana*, auxin transport, GUS expression, pericycle cell, transport direction.

**Introduction**

Higher plants develop various organs after germination i.e., in aerial parts, the shoot meristem produces leaves and stems, while in underground parts, a branching root system is developed through the formation of lateral roots from the primary root. Lateral root (LR) formation is an important developmental process that contributes to the establishment of root conformation to enable the plant to absorb water and nutrients efficiently, and physically to sustain the aerial parts (Park et al. 2005). In *Arabidopsis thaliana*, for example, LRs are generated from several pericycle cells adjacent to the xylem parenchyma, which starts to divide in a highly regulated manner, to form new root tissue toward the lateral axis. The first trigger of cell division at the pericycle leading to LR formation is the entry event of auxin into the cell (Casimiro et al. 2001). Auxin is also deeply involved in vertical axis formation by the polar transport via cell-to-cell movement of indole 3-acetic acid (IAA) in xylem parenchyma cells in plants.

Membrane transport of auxin is regulated by several types of transporters, e.g., PIN proteins (major facilitator superfamily; MFS) and AUX1/LAX $H^+$ symporters (Schnabel and Frugoli 2004; Wiśniewska et al. 2006; Bainbridge et al. 2008; Carraro et al. 2006; Xu et al. 2005). In addition, ATP-binding cassette (ABC) transporters have been discovered as the third major family responsible for the membrane transport of auxin. Out of ca. 120 ABC transporters in a plant, mostly the P-glycoprotein (PGP)/ABCB (hereafter referred to as ABCB) subclass (Jasinski et al. 2003; Verrier et al. 2008) are reported thus far as being relevant for auxin transport (Luschnig 2002; Noh et al. 2001; Noh et al. 2003; Geisler et al. 2005; Terasaka et al. 2005). First, two ABCBs, ABCB1 and ABCB19, in *A. thaliana* were shown to specifically bind the auxin efflux inhibitor 1-N-naphtylphtalamic acid (NPA) (Murphy et al. 2002). T-DNA insertion mutants of *abcb19* showed pleiotropic auxin-related phenotypes and characterization of the double mutant *abcb1*/*abcb19,* and antisense *abcb1* plants strongly suggested that these ABC transporters are necessary for the polar auxin transport.

Previously, we identified another plasma membrane ABCB-type transporter, (PGP4)/ABCB4, in *A. thaliana*, which was specifically expressed in the root epidermis, and demonstrated its involvement in basipetal shoot-ward auxin transport, i.e., from the root tip to the root-shoot transition zone (Terasaka et al. 2005). Most plant ABCB members form pairs sharing high sequence similarity with each other (Geisler and Murphy 2006). The paralog of *ABCB4* in the *Arabidopsis* genome is *ABCB21* (68% nucleotide identity and 79% amino acid identity), but no biochemical and molecular biological characterization was made on this ABCB member. Besides, for ABCB4 conflicting transport directionalities, either inward or outward transport activity, have been reported depending on the experimental systems (Santelia et al.

2005; Terasaka et al. 2005; Lewis et al. 2007; Cho et al. 2007; Kubeš et al. 2012). In this report, we describe the biochemical characterization of ABCB21 comparing the transport property of ABCB4 as well as ABCB1, and suggest that ABCB21 functions as facultative transporter that mediates im- or export of IAA depending on the cytoplasmic IAA concentration.

## Results

### Expression analysis of *ABCB21*

*ABCB21* locates at chromosome 3 and is divided into 11 exons, and the deduced polypeptide consists of 1,293 amino acids (Figure 1a). This ABC protein is grouped in cluster II of the ABCB subfamily, which is separate from cluster I where ABCB1 and ABCB19 are classified (Figure 1b). Due to the high sequence similarity between ABCB4 and ABCB21, a possible transcriptional correlation was evaluated employing a microarray analysis, in which the *abcb4* mutant and wild type *Arabidopsis* were compared (Supplemental Figure S1). In *abcb4*, 158 genes showed a more than 2-fold elevated expression (Supplemental Table S1a), whereas 21 genes revealed less than half that level of expression (Supplemental Table S1b), but no ABC protein genes, including *ABCB21,* were observed in these lists.

To evaluate the organ-specific expression of *ABCB21*, a real-time PCR analysis was conducted indicating that the *ABCB21* transcript was detectable in all *Arabidopsis* tissues examined (Figure 2a). This expression pattern is different from that of *ABCB4* that is almost solely expressed in the root, in particular in the epidermis and the root cap (Terasaka et al. 2005), while strong expression of *ABCB21* was also seen in leaf tissues.

We analyzed the response of *ABCB21* expression to various phytohormones and abiotic stresses using fourteen-day seedlings of *Arabidopsis*. While *ABCB21* expression was decreased upon treatments with benzyladenine, abscisic acid, and gibberelic acid as well as cold or dark treatments, no increase in the gene expression was observed even by auxins at a high concentration in this primary screening (Supplemental Figure S2). However, a time course experiment with a low concentration (300 nM) of IAA showed that the seedlings responded to exogenously added IAA in a different pattern from that of *ABCB4*, i.e., the *ABCB4* expression increased rapidly and then decreased gradually, whereas *ABCB21* expression decreased transiently and then returned to a steady state level gradually (Figure 2b), suggesting a different physiological role of *ABCB21* from that of *ABCB4*.

A detailed cell-type specific expression analysis of *ABCB21* was performed using *ProABCB21: ß-glucuronidase* (*GUS*) transformant at the $T_3$ generation, in which a 0.75 kb sequence upstream of the *ABCB21* initiation codon was fused to a *GUS* reporter gene. The *ProABCB21: GUS* transformants were histochemically stained with X-Gluc at different developmental stages. The promoter length used in this experiment was 0.75 kb, because another gene (At3g62160) was found upstream of the promoter region. At the aerial part, *ABCB21* was expressed in the cotyledon, which was almost specifically located at the abaxial side (Figure 3a-c). Strong expression was also observed at junctions between the cauline leaf

and stem, and the petal and inflorescence stem (Figure 3d-f). Weak expression was seen in vascular tissues in petals (Figure 3g). In young seedlings shortly after hatching, GUS staining was prominent in the boundary regions of hydrathodes of cotyledons (Supplemental Figure S3). The most remarkable cell-type specific expression of *ABCB21* was observed in the root tissue, where GUS staining was restricted to the pericycle; in particular, the strongest staining was seen at the part adjacent to the xylem parenchyma, but not at the root cap (Figure 3h-m). In summary, it appears that despite their high sequence similarity the expression pattern and responsiveness to auxin of *ABCB21* and *ABCB4* are highly complementary.

**Membrane localization of ABCB21**

Membrane localization of ABCB21 was analyzed by sucrose density gradient fractionation of microsomal membranes followed by western blot, in which a specific peptide antibody directed against ABCB21 was used. The ABCB21 polypeptide peaks at the 32/38% fraction that coincides with that of the plasma membrane $H^+$-ATPase AHA, and the fractionation pattern is apparently different from those of the $H^+$-pyrophosphatase (AVP1) and of the ER luminal binding protein (BiP), which were used as markers of vacuolar and endoplasmic reticulum membrane proteins, respectively (Figure 4). These results suggest that ABCB21 is located on the plasma membrane and not on vacuolar membranes or the endoplasmic reticulum.

**ABCB21 is a facultative auxin im/exporter**

To analyze the transport function of ABCB21 *in planta*, we obtained an insertion (WiscDsLox1C2) mutant of the *ABCB21* gene from the Wisconsin mutant collection. However, RT-PCR analysis of mutant seedlings indicated that the transcript corresponding to the 3'-trancated *ABCB21* ORF was clearly detected and the coding sequence for the first ATPase domain remained (Supplemental Figure S4). Adding to the absence of the P-value of this gene in the microarray analysis of the loss-of-function mutant (not shown) and its low germination rate, we did not use the strain for further studies.

As second best option, we therefore generated *ABCB21* RNAi lines, in which an intron-spliced hairpin RNA (RNAi) construct targeted to the *ABCB21* sequence was introduced (Figure 1a). Among eighteen kanamaycin-resistant transformants, two lines, designated *abcb21-ir1* and *abcb21-ir2*, showed strong silencing at the protein level that were used for further studies (Figure 5a). Importantly, in these RNAi lines, ABCB4 expression was not significantly influenced.

Having the proposed import directionality for ABCB4 (Santelia et al. 2005; Terasaka et al. 2005), we performed auxin import and export assays in *ABCB21* RNAi plant (line *ir-1*)

mesophyll protoplasts in the presence of 100 nM external IAA (Figure 5b). Surprisingly, in import assays, the *ABCB21* RNAi line showed significantly increased IAA uptake compared to the vector control, indicating, together with the plasma membrane localization, that the transport directionality of ABCB21 may be pointing outward in *Arabidopsis* protoplasts (Figure 5b). Using NAA double labeling in the same assay, we found no significant difference in NAA loading between the RNAi line (*ir-1*) and the vector control (Figure 5c), which is in-line with the chemical feature of NAA unlike IAA to be able to by-pass carrier-mediated uptake by diffusion (Marchant et al. 1999). However, reduced NAA export capacities have also been recently reported for ABCB4 using tobacco BY2 cells (Kubeš et al. 2012). In agreement with this proposed efflux directionality, the export of IAA by the RNAi line was reduced in export assays where outside concentration of auxins were monitored (Figure 5d), while the transport activity for NAA was not at a significant level (Figure 5e).

The transport activity of ABCB21 for IAA was further investigated at the cellular level in yeast. As previously reported for ABCB1 (Geisler et al. 2005), the plasma membrane localization of ABCB21 expressed in yeast cells was confirmed by membrane fractionation using sucrose density gradient centrifugation followed by western blot analysis (Figure 6a). The IAA-sensitive strain *gef1* (for Glycerol/ethanol Fe-requiring) lacks a putative chloride channel protein. In a growth test using 5-fluoroindole, a toxic analog of a potential IAA precursor, which provides a useful tool for evaluating auxin transport (Gaxiola et al. 1998). ABCB21, like ABCB4 (Santelia et al. 2005) showed a significant hypersensitivity compared to the vector control (Figure 6b), supporting the assumption that ABCB21 like its closest homolog might function as auxin analog importer in yeast.

In order to clarify these at first hand conflicting transport data in more detail, we performed yeast IAA transport studies for ABCB21, in direct comparison with ABCB1 and ABCB4, both as import and export assays. As explained in detail in the Materials & Methods, in import assays external IAA is added at time point 0 resulting in high external IAA but low cytoplasmic auxin concentrations during this assay. In export assays, prior to export IAA loading followed by removal of external IAA is performed resulting in low external but high cytoplasmic auxin levels. In import assays (Figure 7a), as reported ABCB1 clearly reveals efflux activity for IAA, while ABCB21 as well as ABCB4 show uptake activity in this assay. Usage of the unspecific diffusion control, benzoic acid (BA), employed as double labeling in the same assay demonstrated transport specificity of this assay. However, surprisingly in export assays (Figure 7c) all three ABCBs were capable of exporting IAA resulting in lower IAA retentions, which again was not found with the diffusion control, BA.

To test the idea that cytoplasmic IAA concentration indeed alters the transport directionality of ABCB4 and ABCB21, we repeated import assays after pre-loading with IAA. Strikingly, pre-loading with 10 μM IAA at pH 4.5 completely blocked the ABCB4/ABCB21-mediated IAA import to the vector control level (Figure 7b). IAA pre-loading reduced also ABCB1-catalyzed IAA export, which is however most probably caused by competition of unlabeled IAA with radiolabeled IAA. These findings strongly support our hypothesis that internal IAA regulates the transport directionalities of ABCB21 and ABCB4. Interestingly, BA export seems to be reduced in ABCB21- and ABCB4-expressing yeast, despite not significant, arguing that internal IAA might influence the specificity of transport substrates for ABCB21 and ABCB4 (Figure 7b).

Finally, we also tested NPA-binding of those ABCB members. Figure 7d and 7e reveal that all three can bind with NPA to a similar extent, and that NPA suppressed the IAA transport function of ABCB21 as well as of ABCB4 as was reported before for ABCB1 (Geisler et al. 2005).

In summary these data imply that ABCB21, in analogy to its closest homolog, ABCB4, is functioning as NPA-sensitive, plasma membrane-localized auxin transporter. However, in contrast to the strict auxin exporter, ABCB1, the transport directionality of ABCB21 and ABCB4 as im/exporter is facultative and probably determined by cytoplasmic auxin levels.

**Phenotype observation of *abcb21* knockdown mutants**

We have carefully observed to find morphological differences of *abcb*21 RNAi lines compared to wild type plant, especially in the root phenotype. These RNAi liens tend to show retardation at the germination process, but they grow normally and revealed basically no significant morphological differences (Supplemental Figure S5). In 10-day-old seedlings of T3 generation, for example, the main root length of wild type and RNAi line was 22.3 ± 4.8 mm and 21.7 ± 5.5 mm (n=15), respectively, whereas the number of lateral roots was 2.2 ± 1.4 and 2.5 ± 1.8 (n=15) for wild type and RNAi line, respectively. The lack of a visible phenotype for *abcb21* RNAi lines may be a result of the putative functional redundancy of other uncharacterized ABCB transporters expressed in these tissues, or phenotype differences may be only observed under special stress conditions.

**Discussion**

Thus far, membrane transporters of auxin have been studied intensively from the viewpoint of the polar movement of the IAA molecule along the vertical axis of the plant body, to which PIN proteins provide a dominant contribution. Similarly, both ABCB1 and ABCB19, as well as auxin importers of the AUX1/LAX family are also relevant for the down-ward movement of auxin in parenchyma cells. Another ABC protein of the B family, ABCB4, is expressed specifically at the root epidermis, which mediates the up-ward movement of IAA molecule. In this study, we have demonstrated that a new member of ABCB subfamily, *ABCB21*, is expressed in the abaxial side of cotyledon, in junctions of lateral organs in the aerial part, and in pericycle cells adjacent to the protoxylem poles of *Arabidopsis* root, and further this ABC transporter recognized IAA as a transport substrate. Also, this transporter protein binds NPA resulting in inhibition of IAA transport.

The initiation of LR formation process is triggered by the entrance of the IAA molecule from the xylem parenchyma into pericycle cells (Laskowski et al. 1995; Himanen et al. 2002). In the microarray analysis of the *abcb21* RNAi lines, the expression of *LAX3*, *PIN5*, and *SHY2* involved in LR development were significantly down-regulated (Bouchard et al. 2006; Blakeslee et al. 2007) (Supplemental Table S2). We then observed how ABCB21 expression is altered during the LR initiation process with *ABCB21* promoter-GUS transformants (Supplemental Figure S6). At the dividing pericycle cell, *ABCB21* expression disappeared when lateral root initiation occurs, which is the phase II to III according to the literature (Vanneste et al. 2005). This suggests that *ABCB21* may be relevant for lateral root initiation, but once the initiation occurs the role of this transporter can be terminated. We thus expected that knock-down lines show phenotype alterations in root development, but no clear difference was observed (data not shown). This does, however, relative frequently occur in the knock down lines, or even in knock-out mutants of ABC transporter genes, because there is a high redundancy of this gene family in plants. If an uncharacterized transporter of functional redundancy is identified, the double knock-out mutant might provide more informative phenotype as reported for ABCB1 and ABCB19 (Noh, et al., 2001).

The *abcb21* loss-of-function line (Wisconsin No. CS848985) showed a very low germination rate, and germinated plants did not show a clear auxin-related phenotype either, including LR development. This suggests that the main phenotype of *ABCB21* loss-of-function is the failure of seed development, and the minority of seeds that could somehow compensate the ABCB21 function by yet unidentified IAA transporters, can germinate. Thus, we analyzed the biochemical function of ABCB21 in the root using RNAi lines. The possibility cannot be eliminated that the RNAi construct for suppression of *ABCB21* might influence the expression

of other auxin transporters, but at least a microarray analysis of RNAi lines revealed that the expression of other ABC transporters was not strongly influenced. While we could not find phenotype alterations in our experiments, our data strongly support that ABCB21 is a transporter regulating the auxin movement in various tissues.

Conflicting reports on the transport directionality of ABCB4 have been reported (Terasaka et al. 2005; Lewis et al. 2007; Cho et al. 2007). Likewise, the closest ABCB4 homolog, ABCB21, seems to export IAA from mesophyll protoplast but based on yeast assays functions as auxin importer (Figure 5 and 7). One possible explanation for this behavior might be the molecular environment of the assay systems where different endogenous proteins may influence the transport function. For instance, the immunophilin-like protein TWISTED DWARF1 (TWD1) can modulate the function of ABCBs (Geisler et al. 2003; Bouchard et al. 2006), i.e., when co-expressed with *ABCB1*, TWD1 showed an opposite effect on ABCB1-mediated auxin efflux activity in yeast and HeLa cells (Bouchard et al. 2006). As another example, coordinated auxin transport by ABCB–PIN interactions has also been reported (Noh et al. 2003; Blakeslee et al. 2007), i.e., ABCB4 showed different auxin transport directionalities depending on its PIN partner (Cho et al. 2007). Obviously, these interacting partners are absent in the yeast expression system.

In this study carefully comparing ABCB1, B4 and B21 transport activity in yeast, we suggest another mechanism in that the cytoplasmic IAA concentration is a key factor determining the directionality of IAA transport (Figure 5 and 7): when cytoplasmic auxin concentrations are low (ca. fM order) such as in the yeast loading assays that were conducted in the absence of non-labeled IAA, both ABCB21 and B4 unlike ABCB1 import auxin (Figure 7). However, when cytoplasmic auxin concentrations are kept relatively high (ca. nM order), either by addition of non-labeled IAA to the protoplast uptake buffer at time point 0 (Figure 5b) or by yeast loading prior to removal of the extracellular supernatant during the export assays (Figure 7c), both ABCB21 and B4 catalyze in the export direction such as ABCB1. This proposed mechanism is supported by IAA pre-loading experiments that blocked ABCB21 and ABCB4-mediated IAA import (Figure 7b). In that respect ABCB21 resembles ABCB4 as a root-localized auxin efflux transporter with auxin uptake activity at low auxin concentrations (Kubeš et al. 2012).

This model is in-line with the identification of putative cytoplasmic regulatory, structural elements in ABCB4 apparently absent in constitutive exporters, ABCB1 and B19 (Yang and Murphy 2009; Kubeš et al. 2012). Taken together, an ABCB protein may show such plasticity for the transport function depending on its subcellular expression altering cytoplasmic auxin

concentrations. However, at this time point we cannot exclude that additional regulatory components, like protein kinases or protein-protein interactions, further tune ABCB21 directionality (Cho et al. 2007; Yang and Murphy 2009).

## Materials and methods

### Plant Material and Growth Conditions

*Arabidopsis thaliana* plants (ecotype Columbia) were grown on soil in growth chambers with 100 or 120 $\mu mol \cdot m^{-2} \cdot s^{-1}$ light in a 16 h light/8 h dark cycle at 21°C. The sterile growth condition was conducted as described elsewhere (Terasaka et al. 2005). To analyze *ABCB21* expression under various growth regulators, seeds were grown on a nylon mesh (20 μm pore) over the MS medium for 14 d under the same light cycle described above. Roots were subjected to various treatments by gentle transfer of the mesh to the new medium. Treatments were stopped by immediate freezing of seedlings in liquid $N_2$. Sequence data for the genes in this study can be found in the GenBank/EMBL data libraries under the following accession numbers: *PGP/ABCB21* (At3g62150), *PGP/ABCB4* (At2g47000), *ß-tubulin* (At5g12250).

### Cloning of *ABCB21* cDNA

The full-length coding sequence of *ABCB21* cDNA (At3g62150) with 12 bp and 17 bp 5'- and 3'-untranslated regions respectively, was isolated by RT-PCR with two primers, ABCB21-Full-Fw and ABCB21-Full-Rv (Supplemental Table S3). The PCR product was subcloned in the pENTR1A vector (Invitrogen).

### Expression Analysis

Total RNA was isolated with the RNeasy Plant Mini-Kit (Qiagen, Valencia, CA). Reverse transcription was done with SuperScript III reverse transcriptase (Invitrogen, CA), followed by incubation with RNase H (Invitrogen, CA).

Real-time PCR was performed with the Roter-Gene 3000A (Corbett Research, Australia), using Platinum SYBR Green qPCR SuperMix-UDG (Invitrogen, CA) according to the manufacturers' instructions. Briefly, the PCR reaction mixture consisted of a10 ng cDNA template, 5 pmol primers, 1 μl fluorescent probe provided by the above kit, and 12.5 μl Platinum Quantitative PCR SuperMix-UDG in a total volume of 25 μl The standard reaction condition was as follows: 95° C for 10 min, 40 cycles of 95° C for 15 s, 50° C for 30 s, 72° C for 30 s. The primers (ABCB21-RT-Fw and ABCB21-RT-Rv) are listed in Supplemental Table S3. Agarose gel electrophoresis, RNA transfers onto Hybond-N+ membranes (GE healthcare UK Ltd.), and hybridization with the 1.1 kb *ABCB21* fragment (positions +2001 to +3063) were performed using standard procedures. The primers (ABCB21-northern-Fw and ABCB21-northern-Rv) are listed in Supplemental Table S3.

**Promoter:GUS Construct and Tissue-specific Expression**

To create the *ABCB21* promoter: reporter construct (*ProABCB21:GUS*), and two PCR primers flanking the regions from –753 to +15 bp were made (ABCB21Pro-Fw and ABCB21Pro-Rv) (Supplemental Table S3). PCR was performed using genomic DNA as a template and KOD-Plus polymerase (TOYOBO). The PCR product was subcloned into the entry vector pDONR221 to transfer the promoter region of ABCB21 into the binary vector pGWB203 by Gateway system (Invitrogen). BP and LR reactions were performed according to standard procedures. *A. tumefaciens* GV3101 (pMP90) was used for transformation *via* the floral-dip method (Clough and Bent 1998). The $T_2$ generation were histochemically stained to detect GUS activity as described elsewhere (Terasaka et al., 2005). Tissue sections (10 µm thick) embedded in Technovit 7100 (Heraeus Kulzer) were prepared by Leica microtome (RM2155) and observed with a Zeiss microscope (Axioskop2).

**Sucrose density gradient fractionation of plant membranes**

Sucrose gradient fractionation was performed basically according to the method described by van den Brule et al. (2002) with the following modifications: *Arabidopsis* roots (10 g) were homogenized in 3 volumes of 50 mM HEPES-KOH, pH 7.5, 5 mM EDTA, 2 mM DTT, 250 mM sucrose, and 1 mM phenylmethylsulfonyl fluoride using mortar and pestle. The homogenate was centrifuged for 15 min to remove the debris, and the microsomal membrane fraction was collected by ultracentrifugation at 100,000 g for 40 min. The pellet was resuspended in 3 mL of gradient buffer (10 mM Tris-MES, pH 7.0, 1 mM DTT, 250 mM sucrose, and 1 mM phenylmethylsulfonyl fluoride) and centrifuged at 100,000 g for 3 h on a noncontinuous sucrose gradient from 20 to 45% (w/v) in the same buffer using a Beckman SW41Ti rotor. Gradient fractions were collected from the interface between different sucrose concentrations, and used for immunoblot analysis.

**Western blotting**

A keyhole limpet hemocyanin conjugate of an oligopeptide of ABCB21, at position 1 (n-MDSVIESEEGLKVDSPNRAD-c), was injected into rabbits according to a standard protocol (Hayashikasei Co. Ltd.). After the third boost, the antiserum was recovered and used for immunoblot analysis. The immunoblot procedure is as described previously (Yazaki et al. 2006). For each membrane marker, antibodies against plasma membrane $H^+$-ATPase (W1D), vacuolar $H^+$-pyrophosphatase (AVP1) and endoplasmic reticulum luminal BiP, were used. For the western blot of Fig. 5a, we used young whole plants.

**Transport experiments with protoplast**

Intact *Arabidopsis* mesophyll protoplasts were prepared from rosette leaves of plants grown on soil under white light (100 µmol $m^{-2}$ $sec^{-1}$, 8 h light/16 h dark, 22°C), and auxin import and export experiments were performed as described (Geisler et al. 2005). Briefly, intact protoplasts were isolated and loaded by incubation with 1 µl $ml^{-1}$ $^3$H-IAA (specific activity 7.4 $\times 10^{11}$ Bq $mmol^{-1}$, American Radiolabeled Chemicals, St Louis, MO, USA) and 4-$^3$H-1-naphthalene acetic acid (9.3 $\times 10^{11}$ Bq $mmol^{-1}$, American Radiolabeled Chemicals) in the presence of 100 nM IAA on ice. Import was started by incubation at 25°C and halted by silicon oil centrifugation. For export assays, loading was performed for 10 min. on ice allowing equal loading and external radioactivity was removed by percol gradient centrifugation. Export was started by incubation at 25°C and halted by silicon oil centrifugation. Exported/imported radioactivity was determined by scintillation counting of the supernatants/protoplast interfaces and is presented as the relative export/import of the initial export/uptake (export/import prior to temperature incubation).

**Expression of *ABCB21* in yeast and transport assay**

The *ABCB21* cDNA-pENTR1A was transferred into the destination vector, pDR196GW, which has a Gateway cassette (*attR1-CmR*, *ccdB-attR2*) in the yeast shuttle vector pDR196 vector (Rentsch et al. 1995). The resulting plasmid, pDR196GW-ABCB21, was used to transform the yeast *gef1* (Gaxiola et al. 1998) or JK93da (Santelia et al. 2005) strains by the lithium acetate method (Ito et al. 1983). For IAA loading experiments, JK93da transformants were grown to $OD_{600}$ = 1, washed and incubated at 30°C with 1 µl $ml^{-1}$ 5-$^3$H-IAA (specific activity 7.4 $\times 10^{11}$ Bq $mmol^{-1}$, American Radiolabeled Chemicals) and $^3$H-benzoic acid acid (9.3 $\times 10^{11}$ Bq $mmol^{-1}$, American Radiolabeled Chemicals) in SD media (pH 5.5). For IAA efflux experiments, yeast cells were loaded at 0°C for 15 min. with 1 µl $ml^{-1}$ 5-$^3$H-IAA (specific activity 7.4 $\times 10^{11}$ Bq $mmol^{-1}$, American Radiolabeled Chemicals) and $^3$H-benzoic acid acid (9.3 $\times 10^{11}$ Bq $mmol^{-1}$, American Radiolabeled Chemicals) in SD media (pH 4.5), followed by two washing steps. Finally, export was started by 10 min. incubation in SD media (pH 5.5) at 30°C. Aliquots of 1 ml were collected, filtered twice with cold water and retained radioactivity was quantified by scintillation counting. Some import assays were conducted with a pre-loading step with 10 µM IAA for 10 min in SD media (pH 4.5) or in the presence of 10 µM NPA in the loading media. NPA binding experiments were carried out as described in Kim et al. (2010).

### *ABCB21* RNAi Transformants

To prepare the RNAi construct, a gene-specific 240 bp fragment from *ABCB21* cDNA (corresponding to nucleotide positions +1,908 to +2148) was subcloned into the destination vector pGWB80 via the donor vector pDONR221 (Invitrogen). The PCR primers (ABCB21ir-Fw and ABCB21ir-Rv) used are listed in Supplemental Table S3. PCR and *in vitro* BP and LR recombinations were carried out as described above. Kanamycin-resistant $T_2$ plants were used in the experiments.


### Acknowledgments

We would like to thank Dr. W. Frommer (Carnegie Institution, Stanford, CA, USA) for pDR196, Dr. Tsuyoshi Nakagawa (Shimane University) for pGWB vectors, Dr. R.A. Gaxiola (University of Connecticut) for the yeast strain *gef1*, Dr. M. Boutry (Université Catholique de Louvain, Belgium) for anti-$H^+$-ATPase antibodies, Dr. N. Koizumi (Osaka Prefecture University, Japan) for anti-BiP antibodies, Dr. M. H. Sato (Kyoto Prefectural University, Japan) for anti-V-PPase antibodies, Dr Hiroo Fukuda and Dr. Kuninori Iwamoto (The University of Tokyo, Japan) for ABCB21 Gene Chip technical support and V. Vincenzetti (University of Zürich) and L. Charrier (University of Fribourg) for excellent technical support. DNA sequencing was conducted with the Life Research Support Center in Akita Prefectural University.

**References**


Bainbridge, K., Guyomarc'h, S., Bayer, E., Swarup, R., Bennett, M., Mandel, T. and Kuhlemeier, C. (2008) Auxin influx carriers stabilize phyllotactic patterning. *Genes Dev.* 22: 810-823.

Blakeslee, J.J., Bandyopadhyay, A., Lee, O.R., Mravec, J., Titapiwatanakun, B., Sauer, M., Makam, S.N., Cheng, Y., Bouchard, R., Adamec, J., Geisler, M., Nagashima, A., Sakai, T., Martinoia, E., Friml, J., Ann, Peer, W.A. and Murphy, A.S. (2007) Interactions among PIN-FORMED and P-glycoprotein auxin transporters in *Arabidopsis*. *Plant Cell* 19: 131-147.

Bouchard, R., Bailly, A., Blakeslee, J.J., Oehring, S.C., Vincenzetti, V., Lee, O.R., Paponov, I., Palme, K., Mancuso, S., Murphy, A.S., Schulz, B. and Geisler M (2006) Immunophilin-like TWISTED DWARF1 modulates auxin efflux activities of *Arabidopsis* P-glycoproteins. *J. Biol. Chem.* 281: 30603-30612.

Carraro, N., Forestan. C., Canova, S., Traas, J. and Varotto, S. (2006) *ZmPIN1a* and *ZmPIN1b* encode two novel putative candidates for polar auxin transport and plant architecture determination of maize. *Plant Physiol.* 142: 254-264.

Casimiro, I., Marchant, A., Bhalerao, R.P., Beeckman, T., Dhooge, S., Swarup, R., Graham, N., Inzé, D., Sandberg, G., Casero, P.J. and Bennett, M. (2001) Auxin transport promotes Arabidopsis lateral root initiation. *Plant Cell* 13: 843-852.

Cho, M., Lee, S.H. and Cho, H.T. (2007) P-glycoprotein4 displays auxin efflux transporter-like action in *Arabidopsis* root hair cells and tobacco cells. *Plant Cell* 19: 3930-3943.

Clough, S.J. and Bent, A.F. (1998) Floral dip: a simplified method for *Agrobacterium*-mediated transformation of *Arabidopsis thaliana*. *Plant J.* 16: 735-743.

Gaxiola, R.A., Yuan, D.S., Klausner, R.D. and Fink, G.R. (1998) The yeast CLC chloride channel functions in cation homeostasis. *Proc. Natl. Acad. Sci. USA* 95: 4046-4050.

Geisler, M., Kolukisaoglu, H.U., Bouchard, R., Billion, K., Berger, J., Saal, B., Frangne, N., Koncz-Kálmán, Z., Koncz. C., Dudler, R., Blakeslee, J.J., Murphy, A.S., Martinoia, E. and Schulz, B. (2003) TWISTED DWARF1, a unique plasma membrane-anchored immunophilin-like protein, interacts with Arabidopsis multidrug resistance-like transporters AtPGP1 and AtPGP19. *Mol. Biol. Cell.* 14: 4238-4249.

Geisler, M., Blakeslee, J.J., Bouchard, R., Lee, O.R., Vincenzetti, V., Bandyopadhyay, A., Titapiwatanakun, B., Peer, W.A., Bailly, A., Richards, E.L., Ejendal, K.F., Smith, A.P., Baroux, C., Grossniklaus, U., Müller, A., Hrycyna, C.A., Dudler, R., Murphy, A.S. and Martinoia, E. (2005) Cellular efflux of auxin catalyzed by the Arabidopsis MDR/PGP

transporter AtPGP1. *Plant J.* 44: 179-194

Geisler, M. and Murphy, A.S. (2006) The ABC of auxin transport: The role of p-glycoproteins in plant development. *FEBS Lett.* 580:1094-1102.

Himanen, K., Boucheron, E., Vanneste, S., Engler, J.A., Inzé, D. and Beeckman, T. (2002) Auxin-mediated cell cycle activation during early lateral root initiation. *Plant Cell* 14: 2339-2351.

Ito, H., Fukuda, Y., Murata, K. and Kimura, A. (1983) Transformation of intact yeast cells treated with alkali cations. *J. Bacteriol.* 153: 163-168.

Jasinski, M., Ducos, E., Martinoia, E. and Boutry, M. (2003) The ATP-binding cassette transporters: structure, function, and gene family comparison between rice and Arabidopsis. *Plant Physiol.* 131: 1169-1177.

Kim, J.Y., Henrichs, S., Bailly, A., Vincenzetti, V., Sovero, V., Mancuso, S., Pollman, S., Kim, D., Geisler, M. and Nam, H.G. (2010) Identification of an ABCB/P-glycoprotein-specific inhibitor of auxin transport by chemical genomics. *J. Biol. Chem.* 285: 23309–23317.

Kubeš, M., Yang, H., Richter, G.L., Cheng, Y., Młodzińska, E., Wang, X., Blakeslee, J.J., Carraro. N,, Petrášek. J,, Zažímalová, E., Hoyerová, K., Peer, W.A., Murphy, A.S. (2012) The Arabidopsis concentration-dependent influx/efflux transporter ABCB4 regulates cellular auxin levels in the root epidermis. *Plant J.* 69: 640–654.

Laskowski, M.J., Williams, M.E., Nusbaum, H.C. and Sussex, I.M. (1995) Formation of lateral root meristems is a two-stage process. *Development* 121: 3303-3310.

Luschnig, C. (2002) Auxin transport: ABC proteins join the club. *Trends Plant Sci.* 7: 329-332.

Lewis, D.R., Miller, N.D., Splitt, B.L., Wu, G. and Spalding, E.P. (2007) Separating the roles of acropetal and basipetal auxin transport on gravitropism with mutations in two *Arabidopsis multidrug resistance-like* ABC transporter genes. *Plant Cell* 19: 1838–1850.

Mravec, J., Skůpa, P., Bailly, A., Hoyerová, K., Krecek, P., Bielach, A., Petrásek, J., Zhang, J., Gaykova, V., Stierhof, Y.D., Dobrev, P.I., Schwarzerová, K., Rolcík, J., Seifertová, D., Luschnig, C., Benková, E., Zazímalová, E., Geisler, M. and Friml, J. (2009) Subcellular homeostasis of phytohormone auxin is mediated by the ER-localized PIN5 transporter. *Nature* 459:1136-1140.

Marchant, A., Kargul, J., May, S.T., Muller, P., Delbarre, A., Perrot-Rechenmann, C. and Bennett, M.J. (1999) AUX1 regulates root gravitropism in *Arabidopsis* by facilitating auxin uptake within root apical tissues. *The EMBO Journal* 18: 2066-73

Murphy, A.S., Hoogner, K.R., Peer, W.A. and Taiz, L. (2002) Identification, purification, and molecular cloning of N-1-naphthylphthalmic acid-binding plasma membrane-associated

aminopeptidases from Arabidopsis. *Plant Physiol.* 128: 935-950.

Noh, B., Murphy, A.S. and Spalding, E.P. (2001) *Multidrug resistance*-like genes of Arabidopsis required for auxin transport and auxin-mediated development. *Plant Cell* 13: 2441-2454.

Noh, B., Bandyopadhyay, A., Peer, W.A., Spalding, E.P. and Murphy, A.S. (2003) Enhanced gravi- and phototropism in plant mdr mutants mislocalizing the auxin efflux protein PIN1. *Nature* 423: 999-1002.

Park, S., Li, J., Pittman, J.K., Berkowitz, G.A., Yang, H., Undurraga, S., Morris, J., Hirschi, K.D. and Gaxiola, R.A. (2005) Up-regulation of a $H^+$-pyrophosphatase ($H^+$-PPase) as a strategy to engineer drought-resistant crop plants. Proc. *Natl. Acad. Sci. U S A* 102: 18830-18835.

Rentsch, D., Laloi, M., Rouhara, I., Schmelzer, E., Delrot, S. and Frommer, W.B. (1995) *NTR1* encodes a high affinity oligopeptide transporter in *Arabidopsis*. *FEBS Lett.* 370: 264-268.

Santelia, D., Vincenzetti, V., Azzarello, E., Bovet, L., Fukao, Y., Düchtig, P., Mancuso, S., Martinoia, E. and Geisler, M. (2005) MDR-like ABC transporter AtPGP4 is involved in auxin-mediated lateral root and root hair development. *FEBS Lett.* 579: 5399-5406.

Schnabel, E.L. and Frugoli, J. (2004) The *PIN* and *LAX* families of auxin transport genes in *Medicago truncatula*. *Mol. Genet. Genomics* 272: 420-432.

Terasaka, K., Blakeslee, J.J., Titapiwatanakun, B., Peer, W.A., Bandyopadhyay, A., Makam, S.N., Lee, O.R., Richards, E.L., Murphy, A.S., Sato, F. and Yazaki, K. (2005) PGP4, an ATP binding cassette P-glycoprotein, catalyzes auxin transport in *Arabidopsis thaliana* roots. *Plant Cell* 17: 2922-2939.

van den Brûle, S., Müller, A., Fleming, A.J. and Smart, C.C. (2002) The ABC transporter SpTUR2 confers resistance to the antifungal diterpene sclareol. *Plant J.* 30: 649-662.

Vanneste, S., Rybel, B.D., Beemster, G.T.S., Ljung, K., Smet, I.D., Isterdael, G.V., Naudts, M., Iida, R., Gruissem, W., Tasaka, M., Inzé, D., Fukaki, H. and Beeckman, T. (2005) Cell Cycle Progression in the Pericycle Is Not Sufficient for SOLITARY ROOT/IAA14-Mediated Lateral Root Initiation in *Arabidopsis thaliana*. *Plant Cell* 17:3035-3050.

Verrier, P.J., Bird, D., Burla, B., Dassa, E., Forestier, C., Geisler, M., Klein, M., Kolukisaoglu, U., Lee, Y., Martinoia, E., Murphy, A., Rea, P.A., Samuels, L., Schulz, B., Spalding, E., Yazaki, K. and Theodoulou, F.L. (2008) Plant ABC proteins-a unified nomenclature and updated inventory. *Trends Plant Sci.* 13: 151-159.

Wiśniewska, J., Xu, J., Seifertová, D., Brewer, P.B., Růžička, K., Blilou, I., Rouquié, D.,

Benková, E., Scheres, B. and Friml, J. (2006) Polar PIN localization directs auxin flow in plants. *Science* 312: 883.

Xu, M., Zhu, L., Shou, H. and Wu, P. (2005) A *PIN1* family gene, *OsPIN1*, involved in auxin-dependent adventitious root emergence and tillering in rice. *Plant Cell Physiol.* 46: 1674-1681.

Yang, H. and Murphy, A.S. (2009) Functional expression and characterization of Arabidopsis ABCB, AUX 1 and PIN auxin transporters in *Schizosaccharomyces pombe*. *Plant J.* 59:179–191.

Yazaki, K., Yamanaka, N., Masuno, T., Konagai, S., Shitan, N., Kaneko, S., Ueda, K. and Sato, F. (2006) Heterologous expression of a mammalian ABC transporter in plant and its application to phytoremediation. *Plant Mol. Biol.* 61: 491-503.

**Figure Legends**

**Figure 1. Molecular characterization of *ABCB21*.**

(a) Exon-intron structure of *ABCB21* gene. Exons are shown as shaded boxes and sequences coding for two nucleotide-binding domains (NBD) are shown as white boxes. The region used to prepare RNAi construct is indicated with arrowheads.

(b) Phylogenetic tree of *Arabidopsis* ABCB subfamily, which is classified into three clusters. ABCB21 belonging to cluster II is highlighted. Numbers indicate bootstrap values.

**Figure 2. Expression Profile of *ABCB21* in *Arabidopsis*.**

(a) Organ-specific expression of *ABCB21* monitored by real-time RT-PCR. The experiment was repeated three times and error bars indicate standard deviation.

(b) Time course of auxin response of *ABCB21* and *ABCB4* gene expression. Seedlings were treated with 300 nM indole-3-acetic acid, and sampled at 0, 0.5, 1, 3, and 7 days after treatment. Total RNA (10 μg) prepared from whole seedlings was probed with $^{32}$P-labeled *ABCB21* (top panel) and *ABCB4* fragments (middle panel). Loading controls are shown by *ß-actin* (bottom panel). The experiment was repeated twice to yield similar results.

**Figure 3. GUS staining of the root tissues of *ProABCB21*:GUS transformants.**

Transgenic plant was grown on 1/2 MS media containing 1% sucrose and, the plant was stained with X-Gluc for 24 h. (a) GUS activity in *ProABCB21*: *GUS* cotyledons (whole mount). (b) Magnification of (a). (c) Cross section of cotyledon. (d) GUS activity between cauline leaf and stem junction. (e) GUS activity between silique and stem junction. (f) GUS activity between flower and stem junction. (g) GUS activity in the vein of petals. (h) GUS activity in *ProABCB21*: GUS roots (whole mount). (i) Cross section of root. (j) Longitudinal section of root. (k) Enlargement of (i). (l) Representative GUS activity in root tip. (m) Minority of GUS activity manner in root tip. The experiment was repeated three times with similar results. Bars = 100 μm, except for (k) that is 40μm.

**Figure 4. Membrane localization of ABCB21.**

Fractionation of total microsomes from wild type *Arabidopsis* roots was done on a non-continuous sucrose gradient consisting of 0, 20, 32, 38 and 45% (w/v) sucrose. Membrane fractions were collected from the interfaces between different sucrose concentrations and analyzed via SDS-PAGE and protein gel blotting. Blots were probed with antisera against ABCB21, PM $H^+$-ATPase (AHA), vacuolar $H^+$-PPase (AVP1), and endoplasmic reticulum BiP

(BiP)

**Figure 5. Transport assay of ABCB21 knockdown protoplast cells.**

(a) Protein gel blot analyses of *abcb21* RNAi line. The experiment was repeated three times to yield similar results. (b) Import assay: IAA uptake into protoplasts of *abcb21* RNAi line compared with that of vector control. Values are mean activities ± standard errors, four individual measurements (n=4). (c) Import assay: NAA uptake into protoplasts of *abcb21* RNAi line compared with that of vector control. Values are mean activities ± standard errors, four individual measurements (n=4). (d) Export assay: IAA export from protoplasts of *abcb21* RNAi line compared with that of vector control. Values are mean activities ± standard errors, four individual measurements (n=4). (e) Export assay: NAA export from in protoplasts of *abcb21* RNAi line compared with that of vector control. Values are mean activities ± standard errors, four individual measurements (n=4).

**Figure 6. Membrane localization of ABCB21 in yeast and spot assay.**

(a) ABCB21 and ABCB4 co-migrate with PM marker, $H^+$-ATPase, in continous sucrose gradients judged by Western detection. (b) ABCB21 was expressed in 5-fluoroindole (5-FI) sensitive *gef1* mutant strain; ABCB4 was used for comparison. Cells were 5-fold diluted five times, and 5 µl of each dilution were spotted onto SD-URA media plate supplemented with 50 µM 5-FI. Growth at 30°C was assessed after 3-4 days. Assays were performed with three independent transformants.

**Figure 7. Transport assay of ABCB21 in yeast.**

(a, b) Import assay (high external IAA): IAA and diffusion control, BA, was used, and the retention was measured in yeast cells (strain JK93da) expressing ABCB21, and ABCB1 and ABCB4 as controls. (b) Cold IAA (10 µM) was pre-loaded and the import assay was conducted. (e) Export assay (low external IAA): These yeast transformants were pre-treated with IAA on ice and then export activity was measured (see M&M for details). As diffusion control BA is used. (e) Specific binding of NPA to microsomes prepared from yeast expressing ABCB21, ABCB1 or ABCB4. (f) NPA inhibition of IAA retention (import assays) in yeast expressing ABCB21 and its closest homolog, ABCB4. Data shown are mean activities ± standard errors, three to five individual measurements with each 4 replicates. Significant differences to vector control ($p<0.05$) are indicated by asterisks.

**Supplemental Table S1. Microarray analysis of *abcb4* KO mutant.**

(a) Genes whose expression was increased more than 2-fold in *abcb4* mutant are listed.

(b) Genes whose expression was decreased less than half in *abcb4* KO mutant are listed.

**Supplemental Table S2. Microarray analysis of *abcb21* knockdown mutant.**

The representative list of the genes resulting from microarray analysis in *abcb21* RNAi mutant was indicated. NC, not changed; D, decreased.

**Supplemental Table S3. Primer list.**

The small letters are nonnative sequences representing restriction or recombination sites, respectively.

**Supplemental Figure S1. Microarray analysis of *abcb4* KO mutant.**

(a) Scatter plots of color swapping experiment with *abcb4* and wild type *Arabidopsis*.
In total, 18,018 genes showed the Flag P, among which 158 genes showed more than
2-fold higher expression whereas 21 genes less than half expression in *abcb4* mutant.

(b) ABC protein gene showing P-flag (107 out of 124 genes) in *abcb4* mutant are spotted.
*ABCB4* (At2g47000) is indicalted with arrows. Lines are x2, x1, and x1/2.

**Supplemental Figure S2. Expression Profile of *ABCB21* in *Arabidopsis*.**

Response of *ABCB21* expression to various treatments.
Fourteen-day-old seedlings were treated for 24 h with 10 μM 1-naphthaleneacetic acid (NAA),
10 μM 3-indoleacetic acid (IAA), 10 μM 2,4-dichlorophenoxyacetic acid (2,4-D),
10 μM 6-benzyladenine (BA), 10 μM kinetin, 10 μM abscisic acid (ABA),
10 μM gibberellic acid (GA3), 10 μM brassinolide (BL), 100 μM methyl jasmonate (MeJA),
100 μM salicylic acid (SA), or 10 μM stigmasterol (St). Cold (4℃/low light) and dark treatment was also done for 24 h. Cont., untreated control.
Total RNA (8 μg) prepared from whole seedlings was probed with a $^{32}$P-labeled
*ABCB21* fragment (top panel). Loading controls are shown by *ß*-actin (bottom panel).
The experiment was repeated twice with similar results.

**Supplemental Figure S3. GUS staining of Pro*ABCB21*: GUS transfomants.**

Plants of 1 to 2 day old were grown on 1/2 MS media containing 1% sucrose.
Then, the plant sample was stained with X-Gluc for 24 h.

The seed coat were striped under microscopic observation.
(a) Seed germination. (b) 1 day after germination. (c) 2 day after germination.
The experiment was repeated three times with similar results. Bars = 250 μm

**Supplemental Figure S4. Expression analysis of *ABCB21* gene in *abcb21* KO mutant.**
Total RNA was extracted from five germinated seedlings individually, and RT-PCR
was performed.
The used primers for amplifications of *ABCB21* are listed in Supplemental Table S3.
The experiment was repeated four times with similar results.

**Supplemental Figure S5. Wild type and abcb21 RNAi seedlings.**
Seedlings (T3 generation) were grown on 1/2 MS containing 1% sucrose for 10-days.

**Supplemental Figure S6. Lateral root initiation in GUS plant.** (a) Stage IV. The arrows indicate the end to end of the lateral root. (b) Stage VII. The arrows indicate end to end of lateral root. (c) A lateral root meristem is established.

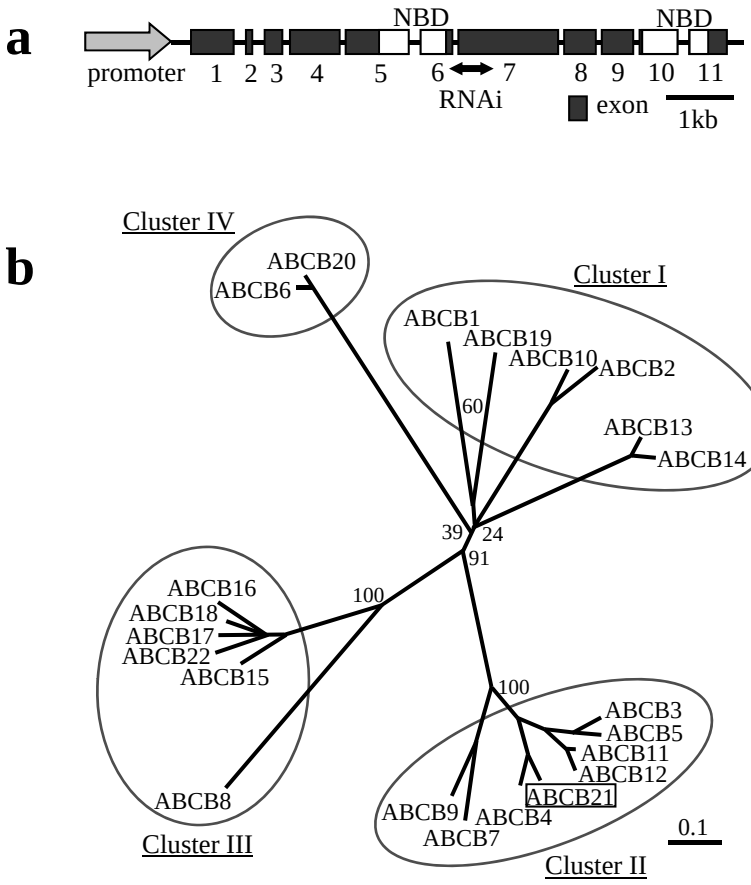


**Kamimoto et al., Figure 1**

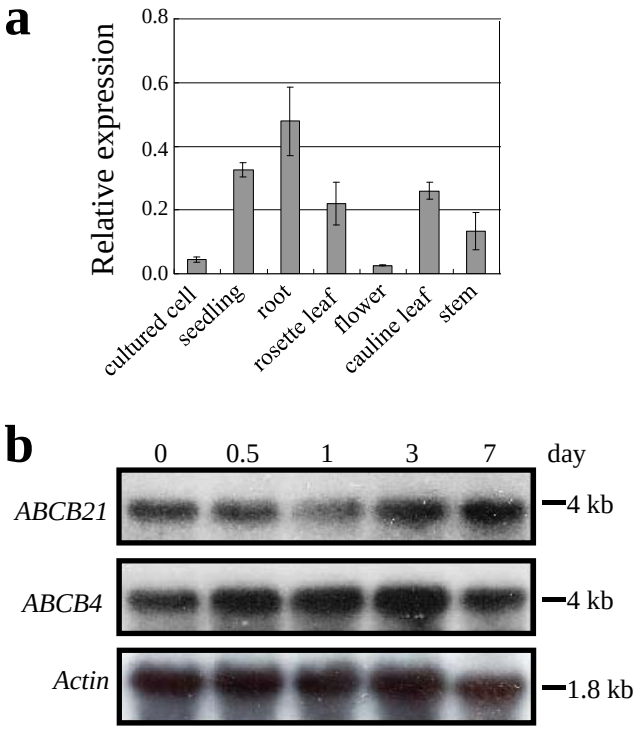


**Kamimoto et al., Figure 2**

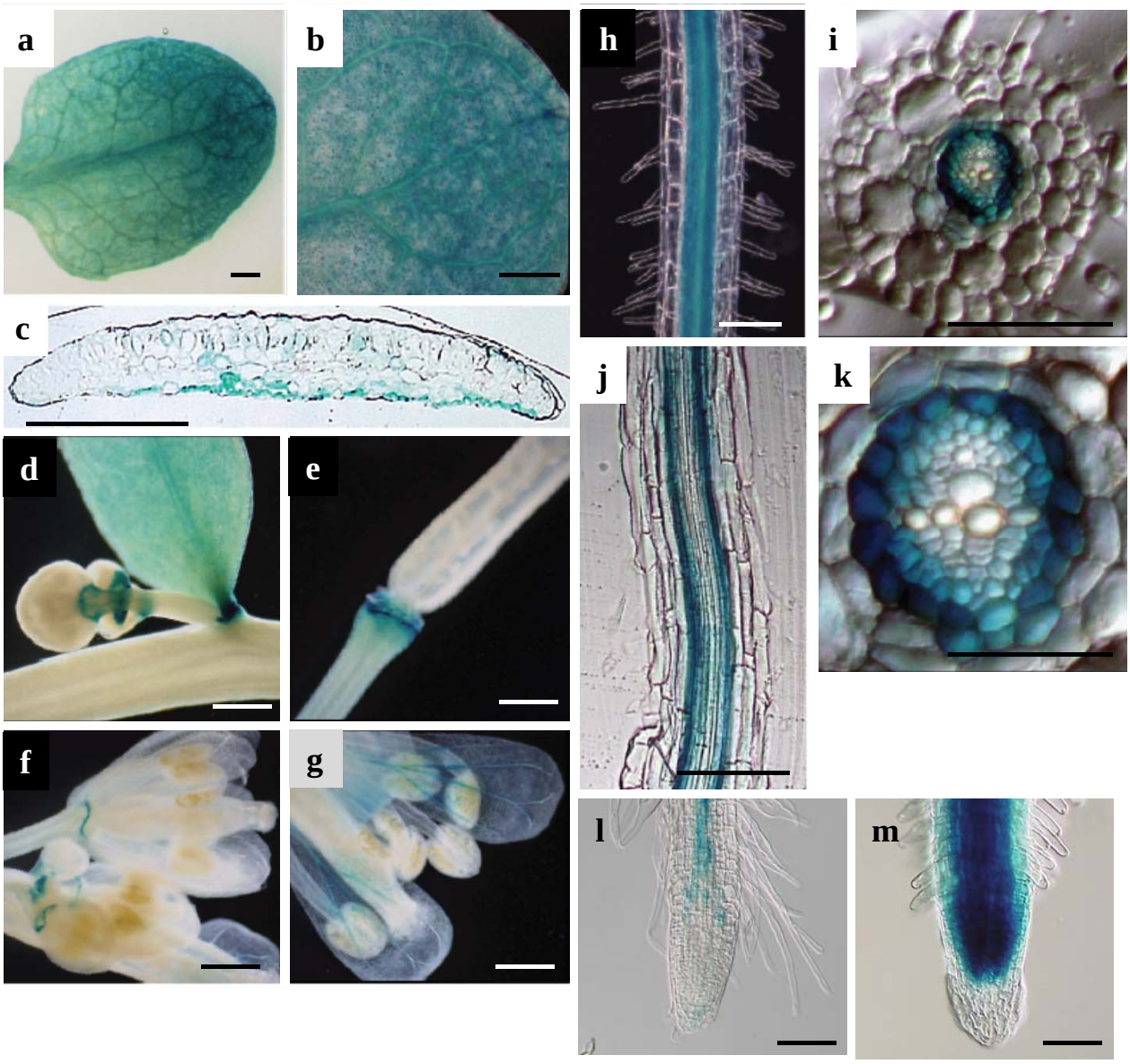


**Kamimoto et al., Figure 3**

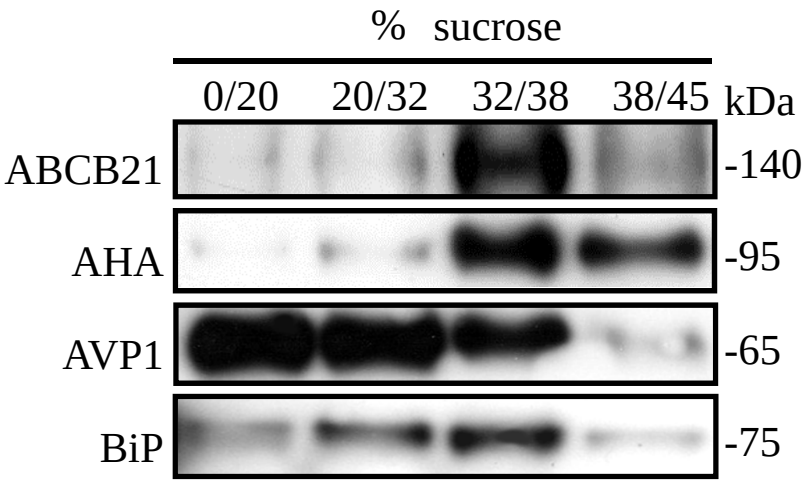


**Kamimoto et al., Figure 4**

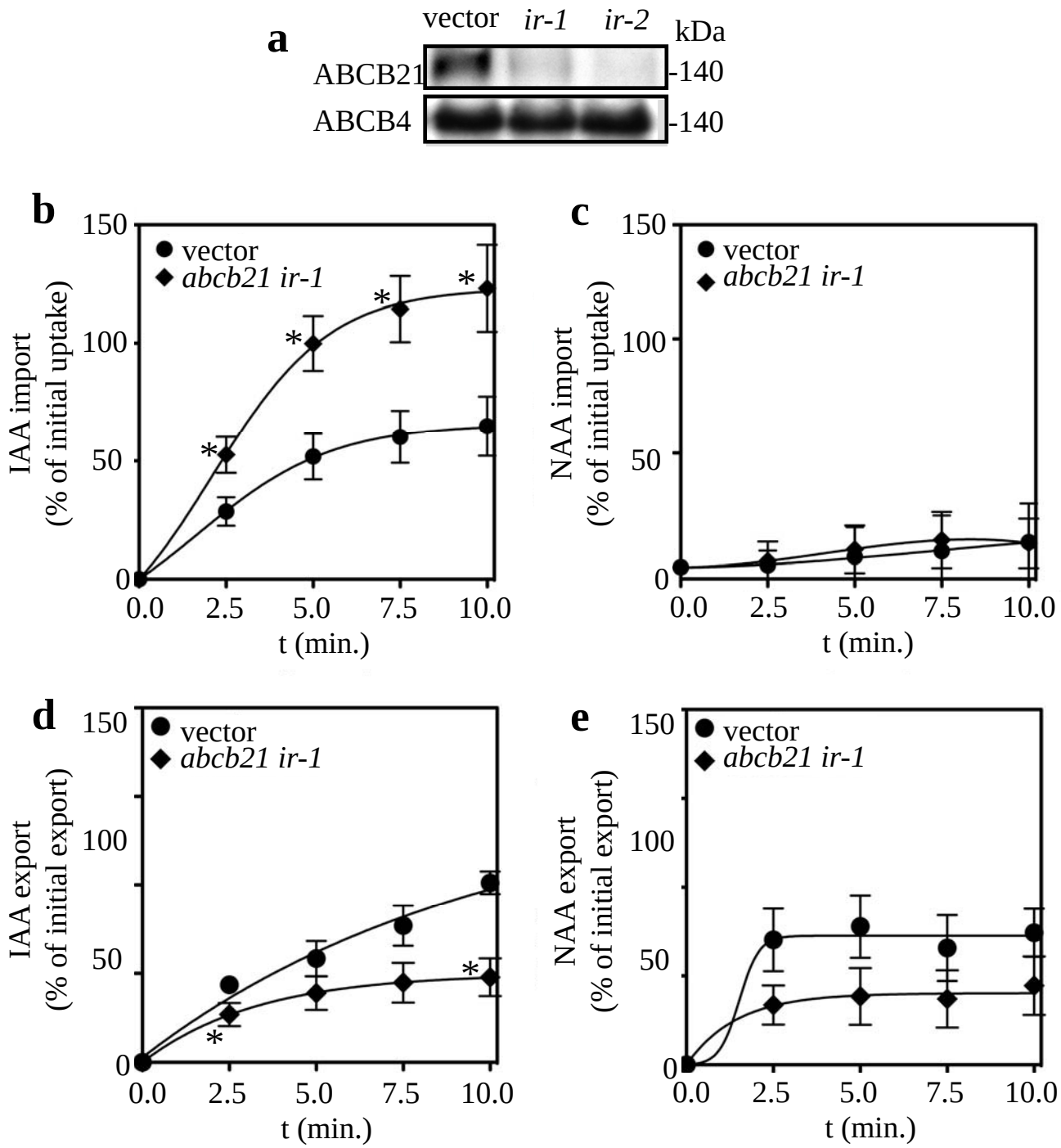


**Kamimoto et al., Figure 5**

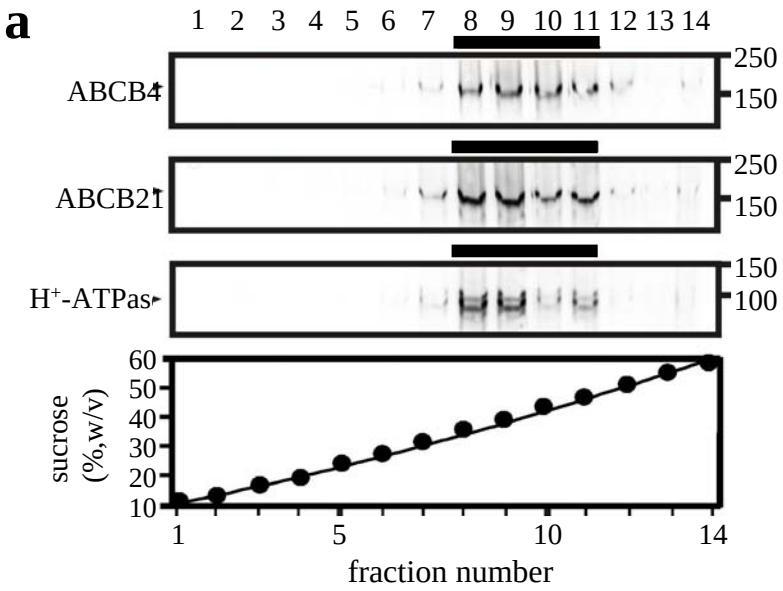


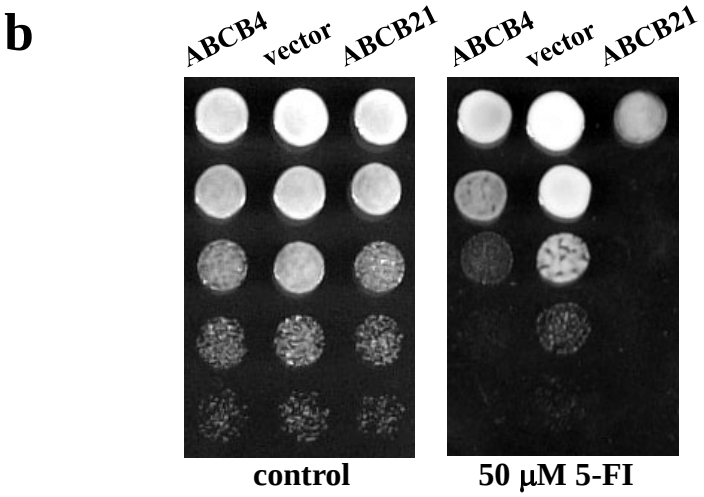


**Kamimoto et al., Figure 6**

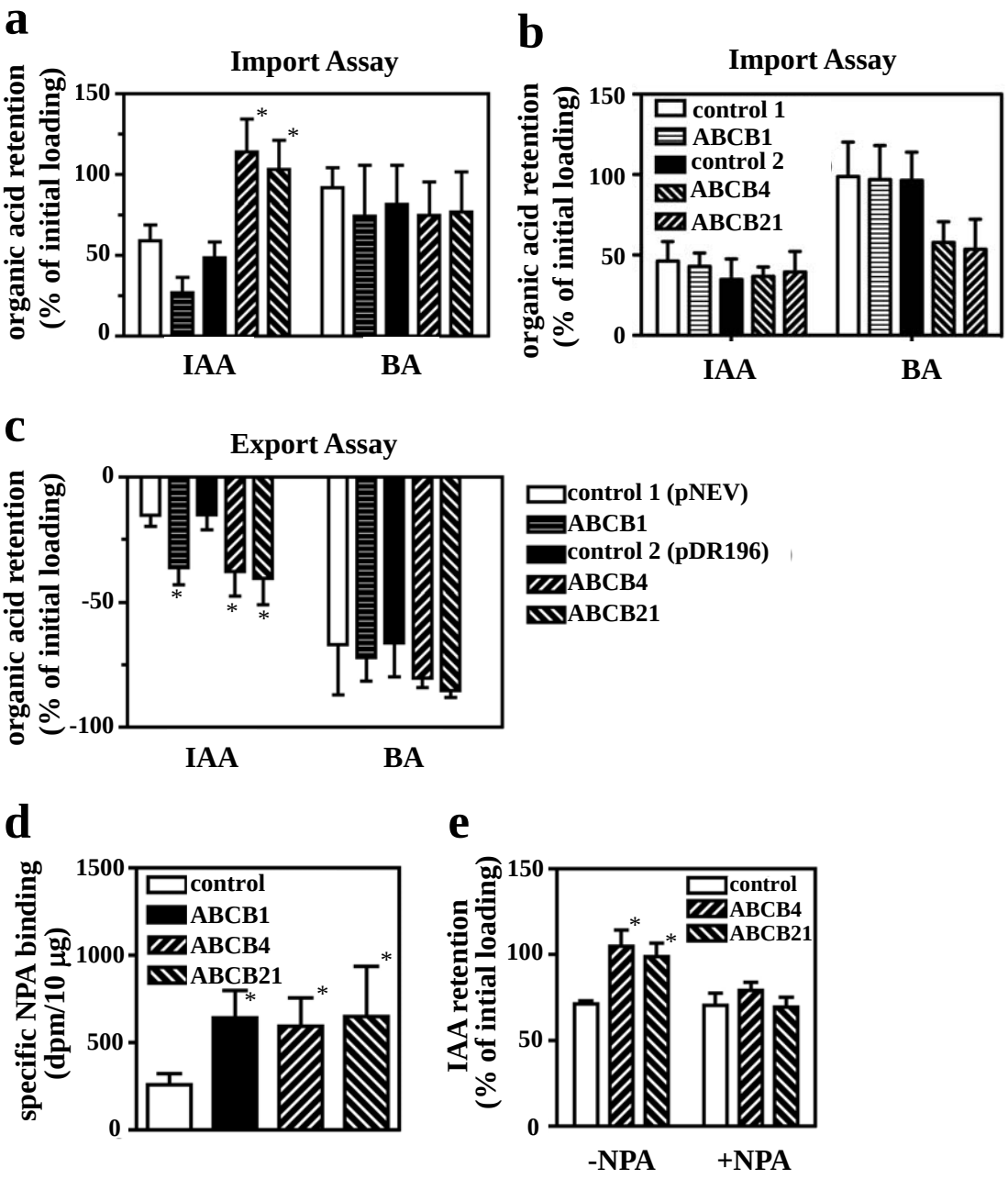


**Kamimoto et al., Figure 7**

**Supplemental Table S1. Microarray analysis of *abcb4* KO mutant.**

(a) Genes whose expression was increased more than 2-fold in *abcb4* mutant are listed.
(b) Genes whose expression was decreased less than half in *abcb4* KO mutant are listed

**a**

| AGI code | Gene name | Fold change (*abcb4* /WT) | Fold change (WT/*abcb4* ) |
|---|---|---|---|
| At1g80840 | WRKY family transcription factor | 21.18 | 0.05 |
| At3g50060 | myb DNA-binding protein (MYB77) | 15.05 | 0.07 |
| At5g57560 | xyloglucan endotransglycosylase (TCH4) | 13.76 | 0.06 |
| At3g55980 | putative protein | 12.90 | 0.08 |
| At4g27280 | putative protein | 12.58 | 0.07 |
| At1g27730 | salt-tolerance zinc finger protein | 11.92 | 0.09 |
| At5g51190 | putative protein | 11.91 | 0.08 |
| At5g45340 | cytochrome p450 family | 10.22 | 0.12 |
| At1g72910 | disease resistance protein (TIR-NBS class), putative | 9.99 | 0.11 |
| At5g61600 | DNA binding protein - like | 9.05 | 0.10 |
| At4g29780 | expressed protein | 8.88 | 0.10 |
| At1g72920 | disease resistance protein (TIR-NBS class), putative | 8.83 | 0.11 |
| At2g40000 | putative nematode-resistance protein | 8.79 | 0.11 |
| At4g11280 | ACC synthase (AtACS-6) | 8.61 | 0.09 |
| At2g41100 | calmodulin-like protein | 8.32 | 0.12 |
| At4g37610 | putative protein | 8.26 | 0.12 |
| At3g44260 | CCR4-associated factor 1-like protein | 7.94 | 0.12 |
| At1g72940 | disease resistance protein (TIR-NBS class), putative | 7.41 | 0.16 |
| At4g24570 | mitochondrial carrier protein family | 7.29 | 0.14 |
| At1g72900 | disease resistance protein (TIR-NBS class), putative | 6.90 | 0.14 |
| At1g73540 | unknown protein | 6.75 | 0.17 |
| At1g21910 | TINY-like protein | 6.34 | 0.25 |
| At3g48360 | putative protein | 6.16 | 0.16 |
| At1g76600 | expressed protein | 6.05 | 0.14 |
| At1g57990 | unknown protein | 5.88 | 0.24 |
| At1g66090 | disease resistance protein (TIR-NBS class), putative | 5.88 | 0.21 |
| At1g68840 | AP2 domain protein RAP2.8 (RAV2) | 5.40 | 0.18 |
| At3g04640 | expressed protein | 5.29 | 0.21 |
| At3g50480 | expressed protein | 5.27 | 0.21 |
| At1g32920 | expressed protein | 5.23 | 0.19 |
| At2g24600 | expressed protein | 5.17 | 0.19 |
| At2g38470 | WRKY family transcription factor | 5.00 | 0.17 |
| At4g23810 | WRKY family transcription factor | 4.98 | 0.17 |
| At4g34150 | putative protein | 4.93 | 0.18 |
| At1g73500 | MAP kinase, putative | 4.91 | 0.26 |
| At5g47230 | ethylene responsive element binding factor 5 (AtERF5) | 4.88 | 0.25 |
| At3g46600 | scarecrow-like protein | 4.87 | 0.22 |
| At5g04340 | putative c2h2 zinc finger transcription factor | 4.84 | 0.20 |
| At1g76650 | putative calmodulin | 4.77 | 0.12 |
| At1g74930 | AP2 domain containing protein, putative | 4.73 | 0.32 |
| At3g56880 | putative protein | 4.71 | 0.22 |
| At5g41750 | disease resistance protein (TIR-NBS-LRR class), putative | 4.69 | 0.24 |
| At2g26530 | AR781, similar to yeast pheromone receptor | 4.65 | 0.24 |
| At4g37290 | expressed protein | 4.59 | 0.48 |
| At3g50800 | putative protein | 4.36 | 0.21 |

**b**

| AGI code | Gene name | Fold change (*abcb4* /WT) | Fold change (WT/*abcb4* ) |
|---|---|---|---|
| At2g47000 | ABC transporter family protein (ABCB4) | 0.18 | 7.30 |
| At1g09350 | putative galactinol synthase | 0.31 | 2.51 |
| At5g48850 | putative protein | 0.31 | 4.00 |
| At4g25480 | DRE binding protein (DREB1A) | 0.31 | 2.70 |
| At5g04120 | phosphoglycerate mutase - like protein | 0.32 | 2.90 |
| At5g20790 | putative protein | 0.33 | 2.64 |
| At2g11810 | putative monogalactosyldiacylglycerol synthase | 0.34 | 2.40 |
| At2g44460 | glycosyl hydrolase family 1 | 0.37 | 3.56 |
| At2g18050 | histone H1 | 0.42 | 2.18 |
| At5g10930 | serine/threonine protein kinase -like protein | 0.43 | 2.06 |
| At2g34210 | putative transcription elongation factor | 0.43 | 2.62 |
| At5g15180 | peroxidase, putative | 0.44 | 2.40 |
| At1g13420 | steroid sulfotransferase, putative | 0.45 | 2.25 |
| At4g26320 | arabinogalactan-protein (AGP13) | 0.45 | 2.62 |
| At1g17710 | hypothetical protein | 0.46 | 2.40 |
| At1g27140 | glutathione transferase, putative | 0.47 | 2.39 |
| At4g11210 | disease resistance response protein family/ dirigent protein family | 0.47 | 2.48 |
| At5g03350 | putative protein | 0.49 | 2.21 |
| At1g52000 | myrosinase binding protein, putative | 0.49 | 2.00 |
| At5g42590 | cytochrome p450, putative | 0.49 | 2.03 |
| At1g23110 | unknown protein | 0.50 | 2.19 |

**Supplemental Table S2. Microarray analysis of *abcb21* knockdown mutant.**

The representative list of the genes resulting from microarray analysis in *abcb21* RNAi mutant was indicated.
NC: not changed. D: decreased.

| AGI code | Gene name | Fold change (*abcb21 ir* /vector control) | Result |
|---|---|---|---|
| At3g62150 | *ABCB21* | -2.83 | D |
| At2g47000 | *ABCB4* | -1.07 | NC |
| At2g36910 | *ABCB1* | -1.07 | NC |
| At3g28860 | *ABCB19* | 1.07 | NC |
| At1g28010 | *ABCB14* | 1.00 | NC |
| At2g38120 | *AUX1* | 1.00 | NC |
| At5g01240 | *LAX1* | 1.00 | NC |
| At2g21050 | *LAX2* | -1.15 | NC |
| At1g77690 | *LAX3* | -1.23 | D |
| At1g73590 | *PIN1* | 1.00 | NC |
| At5g57090 | *PIN2* | 1.00 | NC |
| At1g70940 | *PIN3* | -1.07 | NC |
| At2g01420 | *PIN4* | -1.15 | NC |
| At5g16530 | *PIN5* | -1.74 | D |
| At1g77110 | *PIN6* | 1.15 | NC |
| At1g23080 | *PIN7* | 1.00 | NC |
| At1g04240 | *SHY2/IAA3* | -1.23 | D |

**Supplemental Table S3. Primer list.**
The small letters are nonnative sequences representing restriction or recombination sites, respectively.

| primer name | sequence | Restriction or recombination site |
|---|---|---|
| ABCB21-Full-Fw | ggatccGATCAAAGAACAATGGATAG | BamHI |
| ABCB21-Full-Rv | gaattcGGTGTCAGTTCCATTGTATAGTATTAACTCAG | EcoRI |
| ABCB21-RT-Fw | TCGCTCATACGTCTACAAGAAGATACTAAACAG | - |
| ABCB21-RT-Rv | CGAAAGAGACTTTCTTTTCTTTGATCGG | - |
| ABCB21-northern-Fw | GAGAAAGACATCAAGGTTTCTACTCCG | - |
| ABCB21-northern-Rv | GATCGATGCAGCCGCATTGC | - |
| ABCB21Pro-Fw | gtacaaaaaagcaggctTCTCACTAATCCAGTTTATTAAAATATTGTATAGTG | attB1 |
| ABCB21Pro-Rv | gtacaagaaagctgggtCTATCCATTGTTCTTTGATC | attB2 |
| ABCB21ir-Fw | gtacaaaaaagcaggctTCGCTCATACGTCTACAAGAAGATACTAAACAG | attB1 |
| ABCB21ir-Rv | gtacaagaaagctgggtCGAAAGAGACTTTCTTTTCTTTGATCGG | attB2 |
| f1 | GGATCAAAGAACAATGGATAG | - |
| f2 | TGAGACTGAGAACTCAAGTGGTGCTATTGGA | - |
| r1 | AACAATGAAAGCTAACTGCCAACTC | - |
| r2 | TGTAGAAGCACTCAGATGAAGTTGTA | - |

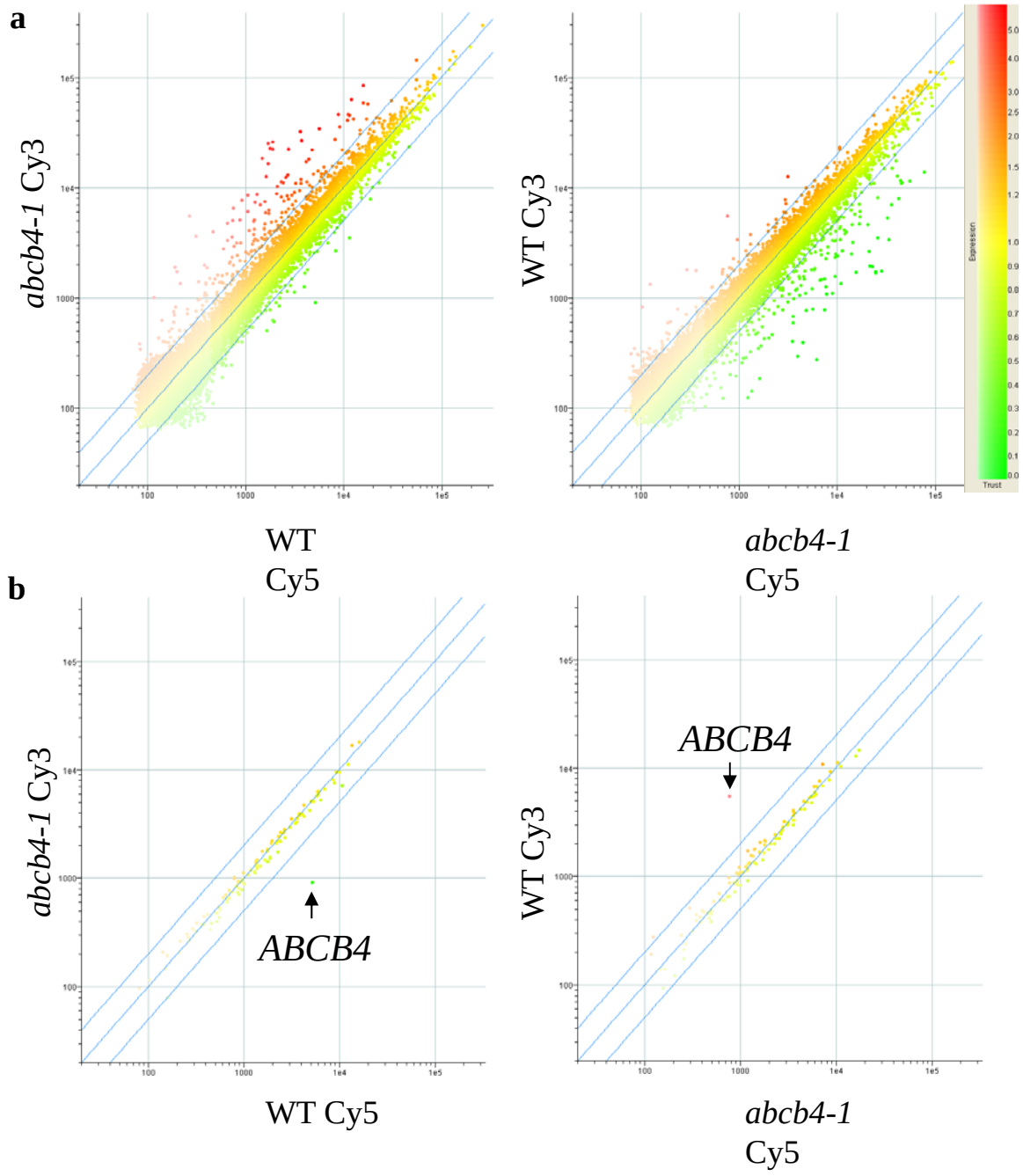


**Supplemental Figure S1. Microarray analysis of *abcb4* KO mutant.**

(a) Scatter plots of color swapping experiment with *abcb4* and wild type *Arabidopsis*. In total, 18,018 genes showed the Flag P, among which 158 genes showed more than 2-fold higher expression whereas 21 genes less than half expression in *abcb4* mutant.
(b) ABC protein gene showing P-flag (107 out of 124 genes) in *abcb4* mutant are spotted. *ABCB4* (At2g47000) is indicalted with arrows.
Lines are x2, x1, and x1/2.

**Kamimoto et al., Figure S1**

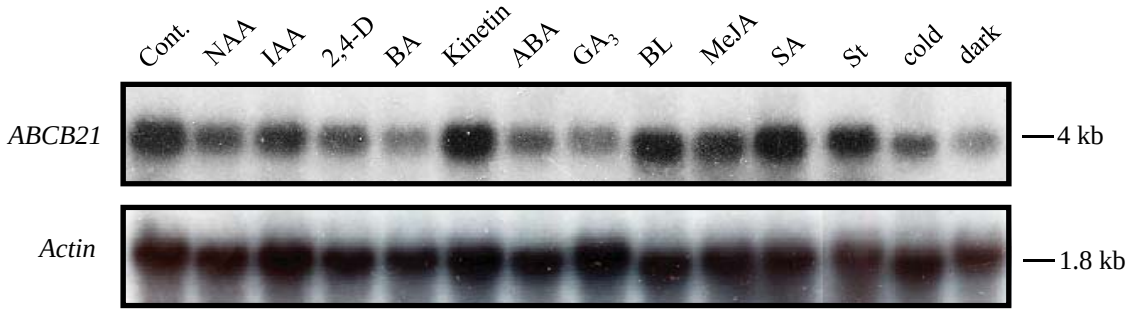


**Supplemental Figure S2. Expression Profile of *ABCB21* in *Arabidopsis*.**

Response of *ABCB21* expression to various treatments.
Fourteen-day-old seedlings were treated for 24 h with 10 µM 1-naphthaleneacetic acid (NAA), 10 µM 3-indoleacetic acid (IAA), 10 µM 2,4-dichlorophenoxyacetic acid (2,4-D), 10 µM 6-benzyladenine (BA), 10 µM kinetin, 10 µM abscisic acid (ABA), 10 µM gibberellic acid (GA3), 10 µM brassinolide (BL), 100 µM methyl jasmonate (MeJA), 100 µM salicylic acid (SA), or 10 µM stigmasterol (St). Cold (4℃/low light) and dark treatment was also done for 24 h. Cont., untreated control.
Total RNA (8 µg) prepared from whole seedlings was probed with a $^{32}$P-labeled *ABCB21* fragment (top panel). Loading controls are shown by *ß-actin* (bottom panel).
The experiment was repeated twice with similar results.

**Kamimoto et al., Figure S2**


**Supplemental Figure S3. GUS staining of *ProABCB21: GUS* transfomants.**

Plants of 1 to 2 day old were grown on 1/2 MS media containing 1% sucrose.
Then, the plant sample was stained with X-Gluc for 24 h.
The seed coat were striped under microscopic observation.
(a) Seed germination. (b) 1 day after germination. (c) 2 day after germination.
The experiment was repeated three times with similar results. Bars = 250 μm

**Kamimoto et al., Figure S3**

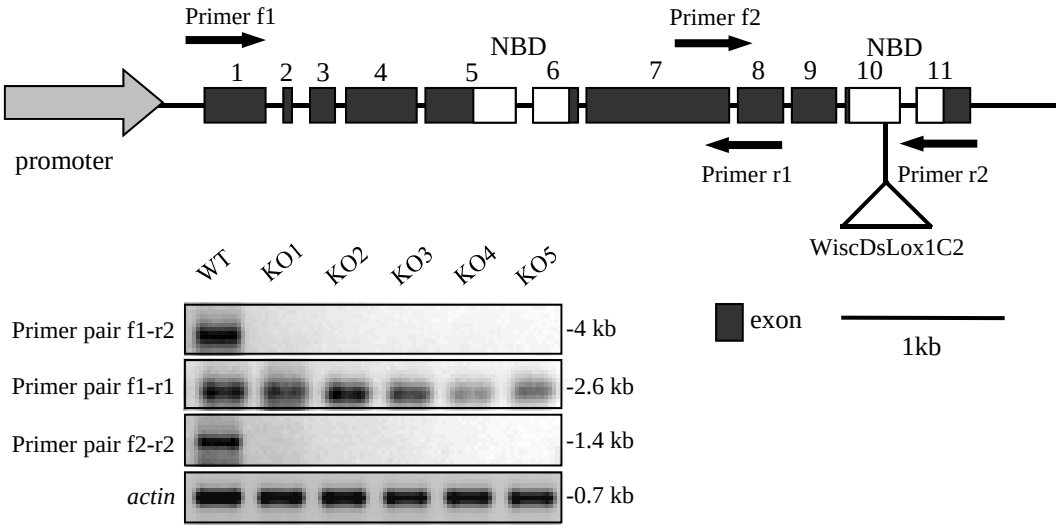


**Supplemental Figure S4. Expression analysis of *ABCB21* gene in *abcb21* KO mutant.**

Total RNA was extracted from five germinated seedlings individually, and RT-PCR was performed.
The used primers for amplifications of *ABCB21* are listed in Supplemental Table S3.
The experiment was repeated four times with similar results.

**Kamimoto et al., Figure S4**

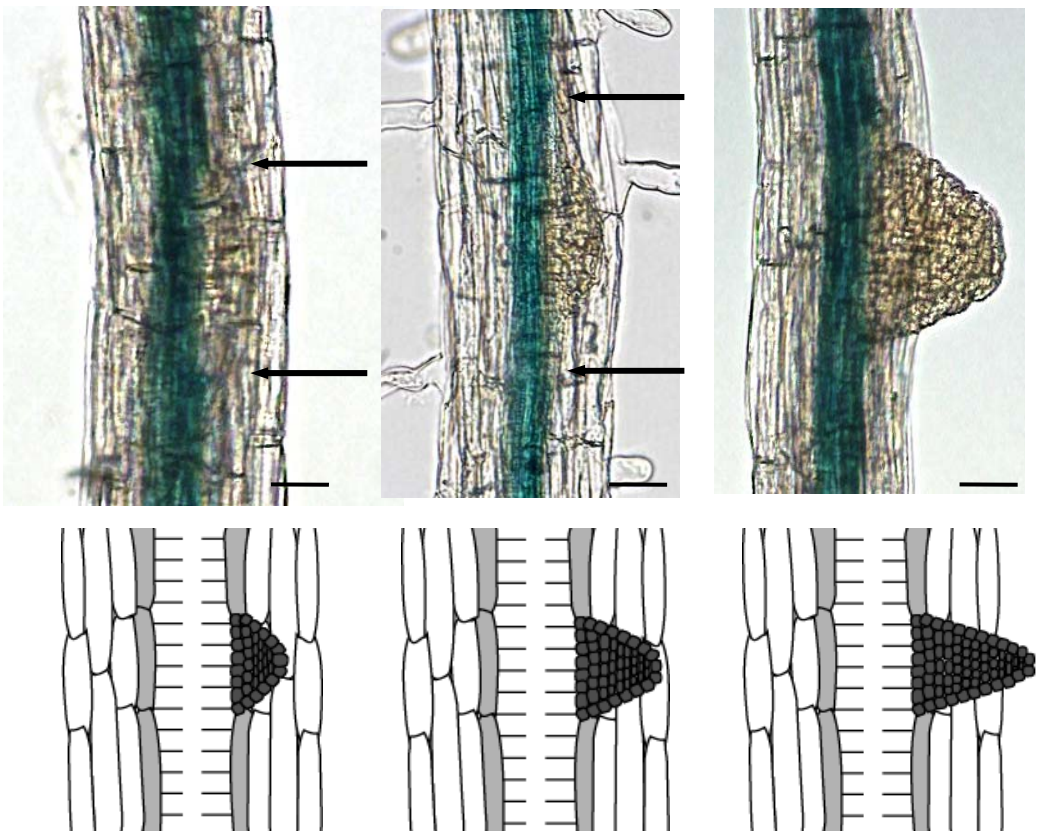

## Supplemental Figure S5. Lateral root initiation in GUS plant

(a) Stage IV. The arrows indicate the end to end of the lateral root.
(b) Stage VII. The arrows indicate end to end of lateral root.
(c) A lateral root meristem is established.

**Kamimoto et al., Figure S5**